Dyes and Pigments 91 (2011) 389–395

Contents lists available at ScienceDirect

Dyes and Pigments

journal homepage: www.elsevier.com/locate/dyepig

Spectroscopic study of anthraquinone dye/amphiphile systems in binary aqueous/organic solvent mixtures

Liang He [a], Harold S. Freeman [b], Lihua Lu [c], Shufen Zhang [a,*]

[a] State Key Laboratory of Fine Chemicals, Dalian University of Technology, Dalian 116012, PR China
[b] Fiber and Polymer Science Program, North Carolina State University, Raleigh, NC 27695-8301, USA
[c] College of Chemistry and Pharmaceutical Sciences, Qingdao Agriculture University, Qingdao 266109, PR China

ARTICLE INFO

Article history:
Received 7 November 2010
Received in revised form
16 April 2011
Accepted 11 May 2011
Available online 25 May 2011

Keywords:
Anthraquinone dyes
Dye/amphiphile system
Solvatochromism
Binary solvent mixture
Solvent polarity
Solvation state

ABSTRACT

The absorption spectra of novel dye/amphiphile systems, in which the dye is a 1,5-*bis*-(R-phenylamino) anthraquinone [R = *o*-methoxy, *o*-ethoxy, H] and the solvents are either organic or H_2O/organic solvent mixtures, have been investigated. It was found that an abrupt λ_{max} shift of more than 80 nm occurred for the system containing dye having R = *o*-methoxy and the amphiphile (poly-bis-(2,2′-dimethyl-5,5′-disulphonate)naphthylmethane disodium salt) in pure solvents with a specific $E_T(30)$ value or in H_2O/DMF (*N*,*N*-dimethylformamide) mixtures containing at least 38% water. This type λ_{max} shift was not observed when solvent mixtures containing the other two dyes were studied. The origin of the pronounced λ_{max} shift is discussed in detail. It is believed that this shift arises mainly from changes in the solvation state of hydrophobic dye having R = *o*-methoxy when water is introduced in the presence of a dispersing agent. In this regard, dye is converted from the monomolecular state to dispersed particles.

1. Introduction

Studies involving solvatochromism and solvatochromic dyes continue to attract attention not only due to academic interest but also because of current and potential utility of such dyes as probes of complex biological systems [1,2] and in chemical sensing [3,4]. The solvatochromic properties of dyes in mixed solvent systems, especially in aqueous binary solutions [5,6], is particularly important since aqueous solvent systems are widely used in reverse phase liquid chromatography and capillary electrophoresis [7]. To date, many papers have been published that outline the spectral band shifts associated with solvatochromic dyes in H_2O containing amphiphiles [8,9], in binary solvent mixtures [10,11], and in mixtures of water and organic solvents [12]. Interestingly, however, the basis for the various spectral band shifts is still a matter of debate [8,12–17].

Regarding amphiphiles themselves, it has long been known that they form aggregates at levels above the critical micelle concentration (cmc) [18]. More recently, experimental evidence for aggregate formation far below the cmc has been demonstrated [19,20]. This phenomenon is known as premicellar aggregation. The resultant metastable aggregates have been investigated using thermodynamic models, to characterize micelles of variable sizes and to calculate their lifetimes [21].

In the present study, the solvatochromic behavior of three novel anthraquinone dye/amphiphile systems (Fig. 1) was examined in a series of pure solvents and binary aqueous solvent mixtures. The present dyes are of interest because it was found during the early stages of this work that an abrupt change in λ_{max} occurred when the proportion of H_2O was varied in H_2O/DMF (*N*,*N*-dimethylformamide) solutions of dye **1** (cf. Fig. 2). Results from experiments undertaken to account for these observations are presented, which include data from scanning electron microscopy and x-ray diffraction studies. Also, using a series of H_2O/organic solvent mixtures, we investigated the relationship between the $E_T(30)$ values of organic solvents and the H_2O content at which there was an abrupt shift in λ_{max} of dye **1**/amphiphile combinations.

2. Experimental section

The dyes used in this study were synthesized according to a published procedure [22]. Before use, the dyes were purified by recrystallization from HOAc. Their melting points were 236–238 °C, 206–208 °C, 199–201 °C, respectively, and are consistent with previous work [23–25]. The amphiphile, poly-bis-(2,2′-dimethyl-

* Corresponding author.
E-mail address: lhedlut2002@yahoo.com.cn (S. Zhang).

0143-7208/$ – see front matter © 2011 Elsevier Ltd. All rights reserved.
doi:10.1016/j.dyepig.2011.05.010

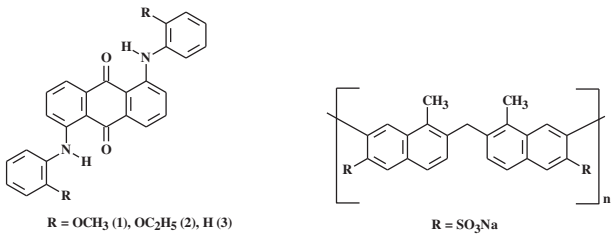

Fig. 1. Molecular structures of the dyes **1**–**3** (left) and amphiphile MF (right).

5,5′-disulphonate)naphthylmethane disodium salt (MF), was purchased from Zhejiang Longsheng Co. (P. R. China) and used without further purification. All solvents were analytical grade and deionized H_2O was used in this study. Filtrations were carried out using a Waters PTFE/silicone syringe filter. The water content was the volumetric ratio. The equilibrium constant was calculated from the ratio of the absorbances, which were proportional to dye concentration.

Absorption spectra were recorded on an HP 8453 UV–visible spectrophotometer, with a wavelength precision of ±0.5 nm. Scanning electron micrographs were obtained using a KYKY-2800B scanning electron microscope (KYKY TECHNOLOGY DEVELOPMENT LTD., P. R. China) operating at 30 kV. Milling of dye and amphiphile MF was carried out with the aid of a mechanical stirrer (60 W) at the desired weight ratio for 6 h. Variation in the ratio of dye to MF was achieved by changing the amount of MF in dye/MF system.

Single crystal formation was achieved by dissolving dye (0.5 g) in acetone (50 mL) at 23 °C (room temperature) and the resulting solution was covered with Parafilm plastic containing pin holes and kept for 1 week, allowing slow evaporation of solvent. A single crystal of dyes **1** and **3** was mounted on a nylon loop using a small amount of Paratone N oil. All X-ray measurements were made on a Bruker-Nonius X8 Apex2 diffractometer at a temperature of 110 K. The unit cell dimensions were determined from a symmetry constrained fit of 9371 (dye **1**) or 6987 (dye **3**) reflections with $4.74° < 2 < 54.37°$ (dye **1**) and $4.94° < 2 < 61.02°$ (dye **3**). The data collection strategy was a number of and scans which collected data up to 72.6° (**2**).

3. Results and discussion

3.1. Absorption spectra

The absorption spectral changes for dyes **1**–**3**/amphiphile MF combinations were studied in pure organic solvents and in aqueous solvent mixtures such as H_2O/DMF, H_2O/ethanol, and H_2O/acetone. It was found that the color of dye **1**/MF (1/3) solutions was red in the less polar pure organic solvents (e.g. THF, acetone) and in the organic solvent-rich binary combinations of H_2O/DMF, but blue in the most polar pure solvents (e.g. ethylene glycol) and in the H_2O-rich binary combinations of H_2O/DMF. Changes in the λ_{max} of dye **1**/MF (1/3) in H_2O/DMF are presented in Fig. 3a. Increasing the proportion of H_2O from 0% to 38% led to an 84 nm λ_{max} increase and a color shift from red to blue. Further increases in H_2O content gave no changes in λ_{max} and the final λ_{max} was essentially the same as that observed in 100% H_2O. With increasing the H_2O content, the absorption spectrum showed a new band as a shoulder at 575 nm. As the proportion of water was increased, the intensity of the shorter-wavelength band decreased and the intensity of the absorption band at 625 nm increased. Also, when the proportion of H_2O was less than 38%, the intensity of the band at 575 nm was higher than the one at 625 nm, but the reverse was the case when the water content was slightly higher than 38%. At 38% water content, the equilibrium constant (Keq) was ~1. Similar results have been reported for a series of 1,4-bis-(alkylamino)anthraquinones in pure solvents, and their short-wavelength bands were attributed to the vibrational overtones of the main peak [26]. The

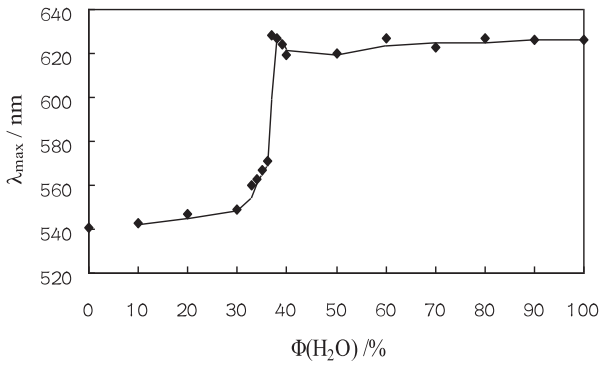

Fig. 2. Effect of water content on λ_{max} (nm) of dye **1**/MF (1/3) in H_2O/DMF mixtures.

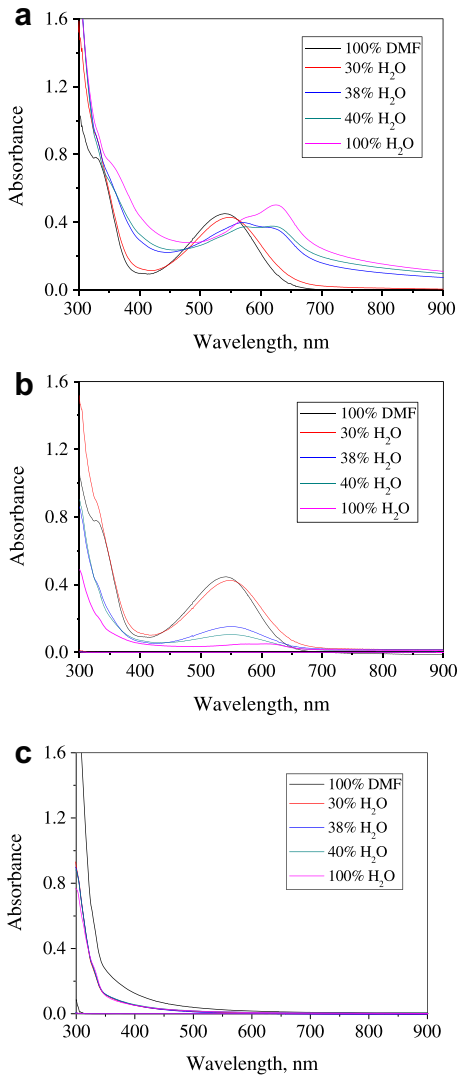

Fig. 3. Absorption spectra of dye **1**/MF (1/3) in H_2O/DMF mixtures, where (a) = dye **1**/MF before filtration with HPLC syringe filter, (b) = dye **1**/MF after filtration, and (c) = MF solutions.

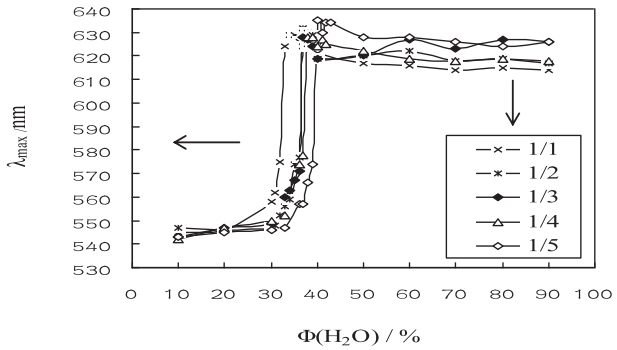

Fig. 4. Influence of dye **1**/MF ratio (1/1–1/5) on λ_{max} in H_2O/DMF mixtures.

present results suggest that the observed color shift arise from changes in the aggregation state of dye **1** when H_2O is added. The addition of H_2O reduced the solubility of hydrophobic dye **1**, increased the solubility of amphiphile MF, and led to the formation of dye **1** dispersed in H_2O in MF micelles. This is best observed in Fig. 3a, where the formation of the band at 575 nm reflects changes in the aggregation state of dye and MF. With this in mind, the solutions were filtered and the spectra recorded again, to give the results shown in Fig. 3b. It can be seen that filtration led to the removal of dispersed dye particles responsible for the absorptions >570 nm and that the intensity of the band at 541 nm reduced significantly when the water content in the solvent mixture increased. Further, the rising baseline in the 700–900 nm region at H_2O levels >30% goes away when dispersed dye particles are removed, as shown in Fig. 3a and b. Using the same concentrations reported in Fig. 3a, the absorption spectra of amphiphile MF in H_2O/DMF mixtures were also recorded (cf. Fig. 3c). The results showed that the amphiphile MF had little effect on the visible absorption spectra of dye **1** but is responsible for absorptions in the 300–350 nm region.

The spectral results from dye **1** are similar to those reported for the absorption properties of medium to long alkyl chain substituted porphyrins in solutions containing surfactant levels below the cmc. The red-shifted Soret band maxima in aqueous-organic media were attributed to porphyrin aggregation and were characterized by band broadening [27]. From studies involving changes in the absorption/emission spectra of Rhodamine 3B perchlorate in toluene/water mixtures, it has been shown that this toluene insoluble ionic dye solubilizes in toluene upon the addition of small

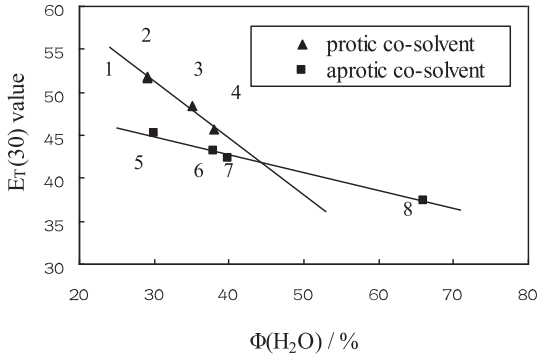

Fig. 5. H_2O content associated with the abrupt λ_{max} shift in H_2O/cosolvent mixtures versus $E_T(30)$ value of the cosolvent, where dye **1**/MF = 1/3 and cosolvents were HOAc (1), ethanol (2), 2-propanol (3), acetonitrile (4), DMSO (5), DMF (6), acetone (7), and tetrahydrofuran (8). Line for protic solvent: $E_T(30) = -0.66\Phi + 71$; line for aprotic solvent: $E_T(30) = -0.21\Phi + 51$.

Table 1
Change in λ_{max} for dye/MF (1/3) as a function of relative solvent polarity.

No.	Solvent	Dye **1**	Dye **2**	Dye **3**	Relative polarity [36]	Dielectric constants [37]
1	Tetrahydrofuran	535	537	529	0.207	7.6[b]
2	Acetone	536	535	527	0.355	20.7[b]
3	DMF	541	542	532	0.404	36.7[b]
4	DMSO	545	544	534	0.444	48.9[a]
5	Acetonitrile	534	534	524	0.460	37.5[a]
6	2-Propanol	538	535	526	0.546	18.3[b]
7	HOAc	538	535	529	0.648	6.2[a]
8	Ethanol	534	534	527	0.654	25.7[a]
9	Ethylene glycol	618	555	537	0.790	38.7[a]
10	H_2O	625	557	538	1.000	80.1[a]
	$\Delta\lambda_{max}$ (nm)	90	20	9		

[a] Values at 20 °C.
[b] Values at 25 °C.

amounts of water. In this case, dye dissolution occurs when the ion pair dissociates into the cationic form with the assistance of diffusing water molecules [28]. These results are consistent with preferential solvation, indicating that local phase separation occurs in the solvation shell.

3.2. Influence of dye 1/MF ratio on λ_{max}

Fig. 4 shows the influence of dye **1**/MF ratio on λ_{max}. It can be seen that changing the ratio from 1/5 to 1/1 decreased the proportion of H_2O in the H_2O/DMF mixture required for an abrupt increase in λ_{max} of the dye solution. When there is $\leq H_2O$ in the solvent medium, dye molecules are largely solvated by organic solvent molecules. For water soluble dyes, the addition of H_2O would lead to displacement of some organic solvent molecules [29] and H-bond formation between dye and H_2O molecules, an important interaction in the first solvation shell [30]. In the present case, it is believed that increasing the MF to dye ratio led to more rapid dispersion of hydrophobic dye **1** in H_2O. This is also consistent with dye aggregation [8,31].

3.3. Relationship between solvent polarity and H_2O content on abrupt λ_{max} change

Absorption spectra for the dye **1**/MF system were measured in a variety of H_2O/organic solvent mixtures, which included protic organic solvents such as ethanol and aprotic organic solvents such as tetrahydrofuran. The results showed that the % H_2O content associated with the abrupt λ_{max} change was influenced by the organic solvent employed, as illustrated in Fig. 5. In this regard, % H_2O content is plotted against $E_T(30)$ values. Since the Reichardt's

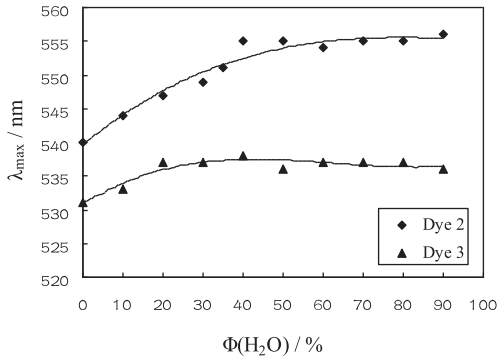

Fig. 6. λ_{max} (nm) changes for dye **2**/MF and dye **3**/MF (1/3) in H_2O/DMF mixtures.

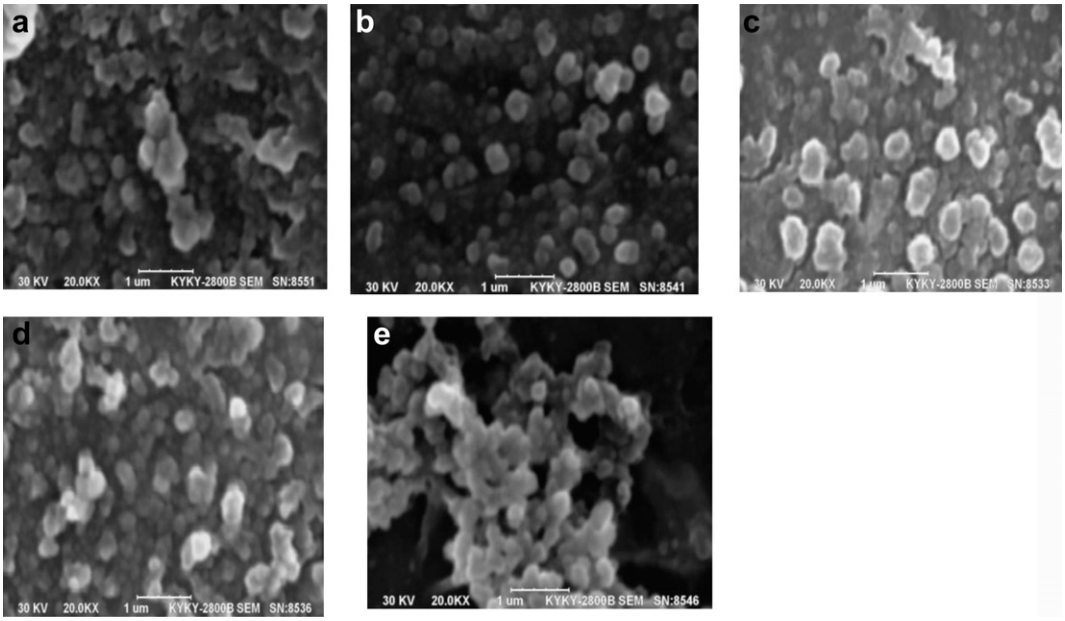

Fig. 7. SEM images of dye **1**/MF (1/3), where C (dye **1**) = 1.33×10^{-4} mol/L in DMF (a), 30/70 H_2O/DMF (b), 38/62 H_2O/DMF (c), 50/50 H_2O/DMF (d), and H_2O (e).

$E_T(30)$ scale is widely used as an empirical description of solvent polarity [32], it was used to assess the solvatochromic properties of the dye 1/MF system. The correlation coefficients for the straight lines obtained were $R^2 = 0.986$ for the series of protic organic solvents and $R^2 = 0.989$ for the aprotic solvents. In these experiments, acetonitrile was treated as a protogenic cosolvent since a strongly basic solute induces the formation of H-bonds [33]. The results obtained in H_2O/acetonitrile fit well with the correlation line derived from the protic solvents. Also, it is clear from the two correlation lines that the H_2O content level at which the abrupt λ_{max} shift occurs decreased with increasing organic solvent polarity. The correlation line for protic solvents had a slope of −0.66, while the slope of the correlation line for aprotic solvents was only −0.21. The slope difference indicates that the solvation of dye **1**/MF in H_2O/protic solvent mixtures was distinct from that in H_2O/aprotic solvent mixtures, which is consistent with the ease of micelle formation in the former type mixtures.

It is well known that absorption band positions can vary with solvent polarity [2,34,35]. Thus, investigation of the absorption spectra of the three dye/MF systems was carried out in solvent media of different polarities, the results of which are shown in Table 1. It is clear from these results that solvents with relative polarity values in the 0.2–0.7 range afforded little change in λ_{max} of each dye/MF system. When relative solvent polarity reached the 0.79 level, however, a small (9 nm) to large (90 nm) solvatochromic effect was observed, with dye **1**/MF giving the most pronounced $\Delta\lambda_{max}$.

3.4. SEM studies

It is clear that the spectral changes associated with dye **2**/MF and dye **3**/MF systems (Fig. 6) were quite different from that for dye **1**/MF under the same conditions. The λ_{max} shifts for dye **2**/MF and dye **3**/MF systems in H_2O/DMF were 16 nm and 6 nm, respectively (Fig. 6), whereas the dye **1**/MF shift was 84 nm. Furthermore, the abrupt λ_{max} shift and the shoulder peaks observed in the absorption spectra of dye **1**/MF did not appear in the absorption spectra from dye **2**/MF and dye **3**/MF. Therefore, to obtain more information about the nature of dye aggregates obtained, combinations of dye **1**/MF containing various H_2O levels were studied using scanning electron microscopy (SEM) (Fig. 7). In Fig. 7a–d dye aggregate sizes were about 300–400 nm but in 100% H_2O (Fig. 7e) they were

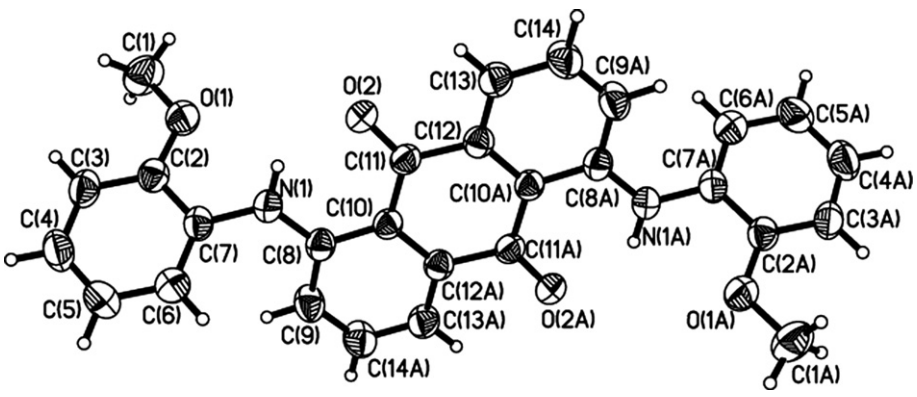

Fig. 8. Single crystal x-ray structure measured for dye **1**.

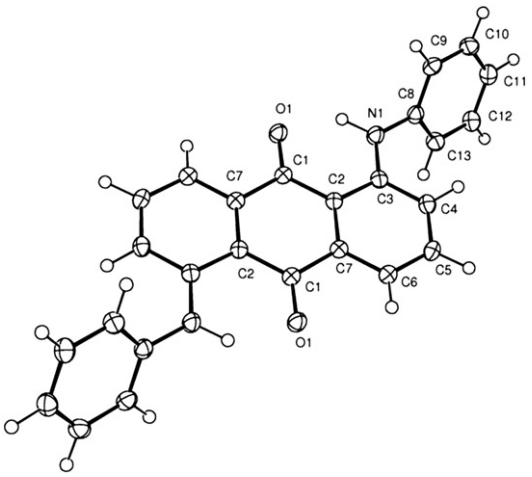

Fig. 9. Single crystal x-ray structure measured for dye **3**.

significantly larger (600–1000 nm). Similarly, there was a bathochromic shift in λ_{max} associated with the changes in aggregate sizes when comparing the sample giving Fig. 7a versus Fig. 7c, while no λ_{max} shift was associated with aggregate formation affording Fig. 7d and e samples.

3.5. X-ray studies

It is interesting to note that the presence of an alkoxy group in the *ortho*-position of the anilino groups of the title dyes afforded a more pronounced solvatochromic affect than when an H-atom occupied that position. Further, the methoxy group had a significantly greater affect than ethoxy. The latter observation led to examination of the x-ray crystal structures of dyes **1** and **3**. It was anticipated that the presence of an *ortho*-methoxy group could produce a bifurcated H-atom, having H-bonding with the O-atoms of the adjacent carbonyl and methoxy groups, promoting a more planar structure. Results obtained for the crystal structure of dye **1** (Fig. 8) showed that the inter-atomic distances for O(1)–N(1) and O(2)–N(1) are 2.477 Å and 1.960 Å, respectively, indicating that both units were within the typical H-bonding distance. The resultant structure would promote co-planarity and aggregation. For dye **3** (Fig. 9), the O(2)–N(1) distance is 1.829 Å. Key bond lengths, bond angles, torsion angles, and detailed crystal data for the two dyes are listed in Tables 2–4, where it can be seen, for instance, that atoms comprising the N(1)–C(7)–C(2)–O(1) moiety of dye **1** lie essentially in the same plane, and there are little differences between bond lengths and angles in the two dye structures.

While the x-ray crystal structure of dye **2** was not solved, it is believed that the observed $\Delta\lambda_{max}$ was influenced by the increased size of the alkoxy group, which adversely affects intramolecular H-bonding and aggregation. On the other hand, dye **3** lacks an alkoxy group altogether, which suggests that the formation of intramolecular H-bonds between the alkoxy groups and the N–H group plays an important role in the magnitude of the spectral band shift of the anthraquinone dye/amphiphile system.

Table 3
Summary of crystal data for dye **1**.

Formula	$C_{21}H_{15}NO_3$
Formula weight (g/mol)	329.34
Crystal dimensions (mm)	0.40 × 0.30 × 0.14
Crystal color and habit	Red prism
Crystal system	Monoclinic
Space group	$P\,2_1/c$
Temperature, K	110
a, Å	11.4222(3)
b, Å	7.9878(2)
c, Å	16.9332(4)
α,°	90.00
β,°	100.9851(12)
γ,°	90.00
V, Å3	1516.65(7)
Number of reflections to determine final unit cell	8857
Min and Max 2θ for cell determination, °	5.66, 63.44
Z	4
$F(000)$	688
ρ (g/cm)	1.442
λ, Å, (MoKα)	0.71070
μ, (cm^{-1})	0.097
Diffractometer type	Bruker–Nonius X8 Apex2
Scan type(s)	phi scans
Max 2θ for data collection, °	69.8
Measured fraction of data	0.847
Number of reflections measured	32405
Unique reflections measured	5620
R_{merge}	0.0308
Number of reflections included in refinement	5620
Cut off threshold expression	>2sigma(I)
Structure refined using	Full matrix least-squares using F^2
Weighting scheme	calc $w = 1/[\text{sigma}^2(F_o^2) + (0.0934P)^2 + 0.1215P]$ where $P = (F_o^2 + 2F_c^2)/3$
Number of parameters in least-squares	286
R_1	0.0517
wR_2	0.1431
R_1 (all data)	0.0803
wR_2 (all data)	0.1608
GOF	1.050
Maximum shift/error	0.001
Min and max peak heights on final ΔF Map (e^-/Å)	−0.204, 0.488

Where: $R_1 = \Sigma(|F_o| - |F_c|)/\Sigma\, F_o$.
$wR_2 = [\Sigma(w(F_o^2 - F_c^2)^2)/\Sigma(wF_o^4)\,]^{½}$.
GOF = $[\Sigma(w(F_o^2 - F_c^2)^2)/(\text{No. of reflns.} - \text{No. of params.})]^{½}$.

Table 2
Key bond lengths and angles for dyes **1** and **3**.[a]

Bond lengths (Å)			Bond angles (°)			Torsion angles (°)		
	Dye **1**	Dye **3**		Dye **1**	Dye **3**		Dye **1**	Dye **3**
O1–C2	1.364	–	O1–C2–C7	115.3	–	O2–C11–C10–C12 (O1–C1–C2–C7)	173.7	176.3
C2–C7 (C8–C9)	1.401	1.379	C6–C7–N1 (C13–C8–N1)	123.1	120.2	O2–C11–C10–C8 (O1–C1–C2–C2)	5.1	−2.1
C7–N1 (C8–N1)	1.410	1.427	C2–C7–N1 (C9–C8–N1)	118.0	119.3	C11–C10–C8–N1 (C1–C2–C3–N1)	2.0	−2.3
N1–C8 (N1–C3)	1.366	1.362	N1–C8–C10 (N1–C3–C2)	120.8	120.8	C7–N1–C10–C9 (C8–N1–C3–C4)	−9.4	7.2
C8–C10 (C3–C2)	1.424	1.426	N1–C8–C9 (N1–C3–C4)	120.8	121.0	C8–N1–C7–C2 (C3–N1–C8–C9)	136.3	−120.3
C10–C11 (C2–C1)	1.457	1.463	C10–C11–O2 (C2–C1–O1)	122.2	122.5	C8–N1–C7–C6 (C3–N1–C8–C13)	−47.2	61.8
C11–O2 (C1–O1)	1.236	1.234	C2–O1–C1	117.8	–	N1–C7–C2–O1	−2.0	–

[a] Information in (·) is for corresponding bonds and angles in dye structure for dye **3**.

Table 4
Summary of crystal data for dye **3**.

Formula	$C_{26}H_{18}N_2O_2$
Formula weight (g/mol)	390.42
Crystal dimensions (mm)	$0.38 \times 0.12 \times 0.06$
Crystal color and habit	Red prism
Crystal system	Monoclinic
Space group	$P\,2_1/n$
Temperature, K	110
a, Å	9.2227(6)
b, Å	4.8368(3)
c, Å	20.7231(14)
α, °	90.00
β, °	92.960(4)
γ, °	90.00
V, Å^3	923.19(10)
Number of reflections to determine final unit cell	6987
Min and Max 2θ for cell determination, °	4.94, 61.02
Z	2
$F(000)$	408
ρ (g/cm)	1.405
λ, Å, (MoKα)	0.71070
μ, (cm^{-1})	0.090
Diffractometer type	Bruker-Nonius X8 Apex2
Scan type(s)	Omega and phi scans
Max 2θ for data collection, °	55.02
Measured fraction of data	0.999
Number of reflections measured	2131
Unique reflections measured	2131
R_{merge}	0.0000
Number of reflections included in refinement	2131
Cut off threshold expression	>2sigma(I)
Structure refined using	Full matrix least-squares using F^2
Weighting scheme	Calc $w = 1/[\text{sigma}^2(F_o^2) + (0.1159P)^2 + 0.6103P]$ where $P = (F_o^2 + 2F_c^2)/3$
Number of parameters in least-squares	173
R_1	0.0588
$wR2$	0.1840
R_1 (all data)	0.0687
wR_2 (all data)	0.1909
GOF	1.067
Maximum shift/error	0.000
Min and Max peak heights on final ΔF map (e^-/Å)	−0.251, 0.325

Where: $R_1 = \Sigma(|F_o| - |F_c|)/\Sigma F_o$.
$wR_2 = [\Sigma(w(F_o^2 - F_c^2)^2)/\Sigma(wF_o^4)]^{1/2}$.
$\text{GOF} = [\Sigma(w(F_o^2 - F_c^2)^2)/(\text{No. of reflns.} - \text{No. of params.})]^{1/2}$.

4. Conclusions

The effects of solvents on the absorption spectra of 1,5-bis-(2-methoxyanilino)-anthraquinone/amphiphile systems were investigated, to account for the abrupt and pronounced λ_{max} change ($\Delta\lambda_{max} > 80$ nm) when this dye was dissolved in certain solvents. Using a series of organic solvents and binary mixtures of those solvents with H_2O, it was found that the abrupt change in λ_{max} occurred when the relative polarity value of the solvents reached 0.79. Also, in H_2O/organic solvent mixtures, an abrupt λ_{max} change occurred at varying water contents, with the more polar solvents requiring less H_2O to afford a pronounced λ_{max} shift. Similarly, increasing the ratio of dispersing agent (amphiphile MF) to anthraquinone dye increased the proportion of H_2O required in H_2O/organic solvent mixtures to give an abrupt λ_{max} change. Examination of absorption spectral data in tandem with SEM and x-ray analyses indicated that the λ_{max} change arises from changes in the solvation state of the dye when H_2O is introduced. In this regard, the dye is converted from the monomolecular state in various organic solvents to dispersed particles in aqueous media.

Acknowledgment

This research was supported by the National Natural Science Funds for Distinguished Young Scholar of China (No.20525620) and China Scholarship Council (No.2007102249).

References

[1] Guzow K, Szabelski M, Karolczak J, Wiczk W. Solvatochromism of 3-[2-(aryl) benzoxazol-5-yl]alanine derivatives. Journal of Photochemistry and Photobiology A 2005;170:215–23.
[2] Masternak A, Wenska G, Milecki J, Skalski B, Franzen S. Solvatochromism of a novel betaine dye derived from purine. The Journal of Physical Chemistry A 2005;109:759–66.
[3] Meinershagen JL, Bein T. Optical sensing in nanopores. Encapsulation of the solvatochromic dye Nile Red in zeolites. Journal of the American Chemical Society 1999;121:448–9.
[4] Herodes K, Leito I, Koppel J, Reichardt C, Koppel IA. UV–Vis spectroscopic study of the hydrophilic and solvatochromic 4-[2,6-diphenyl-4-(pyridin-4-yl) pyridinium-1-yl]-2,6-bis(pyridin-3-yl)phenolate betaine dye in aqueous tetra-n-butylammonium bromide. Journal of Physical Organic Chemistry 2005;18:1013–7.
[5] Hisamoto H, Tohma H, Yamada T, Yamauchi K, Siswanta D, Yoshioka N, Suzuki K. Molecular design, characterization, and application of multi-information dyes for multi-dimensional optical chemical sensing. Molecular design concepts of the dyes and their fundamental spectral characteristics. Analytica Chimica Acta 1998;373:271–89.
[6] Tada EB, Silva PL, El Seoud OA. Thermo-solvatochromism of betaine dyes in aqueous alcohols: explicit consideration of the water-alcohol complex. Journal of Physical Organic Chemistry 2003;16:691–9.
[7] Peyrin E, Peyrin FX, Guillaume YC. Retention behavior modelization of monoprotic and diprotic species in a hydroorganic acetonitrile/water mixture. Analytical Chemistry 1999;71:2708–13.
[8] Buwalda RT, Jonker JM, Engberts JBFN. Aggregation of azo dyes with cationic amphiphiles at low concentrations in aqueous solution. Langmuir 1999;15:1083–9.
[9] Mchedlov-Petrossyan NO, Vodolazkaya NA, Kornienko AA, Karyakina EL, Reichardt C. Langmuir 2005;21:7090–6.
[10] Wetzler DE, Chesta C, Fernández-Prini R, Aramendia PF. Dynamic solvation of aminophthalimides in solvent mixtures. The Journal of Physical Chemistry A 2002;106:2390–400.
[11] Martins CT, Lima MS, El Seoud OA. A novel, convenient, quinoline-based merocyanine dye: probing solvation in pure and mixed solvents and in the interfacial region of an anionic micelle. Journal of Physical Organic Chemistry 2005;18:1072–85.
[12] Gameiro P, Pereira E, Garcia P, Breia S, Burgess J, de Castro B. Derivatives of bis(2,2′-bipyridyl)dicyanoiron(II) with long alkyl chains- versatile solvatochromic probes that form metalloaggregates in water-rich media. European Journal of Inorganic Chemistry 2001;11:2755–61.
[13] Quadrifoglio F, Crezenzi V. The interaction of methyl orange and other azo-dyes with polyelectrolytes and with colloidal electrolytes in dilute aqueous solution. Journal of Colloid and Interface Science 1971;35:447–59.
[14] Masoud MS, Ali AE, Shaker MA, Ghani MA. Solvatochromic behavior of the electronic absorption spectra of some azo derivatives of amino pyridines. Spectrochimica Acta Part A 2004;60:3155–9.
[15] Zoon PD, Brouwer AM. Paradoxical solvent effects on the absorption and emission spectra of amino-substituted perylene monoimides. ChemPhysChem 2005;6:1574–80.
[16] Takagishi T, Ueno T, Kuroke N, Shima S, Sakai H. Interaction of α-poly-L-lysine and ε-poly-L-lysine with methyl orange and its homologs in aqueous solution: Results from dialysis and spectraoscopic measurements. Journal of Polymer Science: Polymer Chemistry Edition 1984;22:1281–9.
[17] Dutta RK, Bhat SN. Interaction of methyl orange with submicellar cationic surfactants. Bulletin of the Chemical Society of Japan 1993;66:2457–60.
[18] Israelachvili JN, Mitchell DJ, Ninham BW. Theory of self-assembly of hydrocarbon amphiphiles into micelles and bilayers. Journal of the Chemical Society, Faraday Transactions 1976;72:1525–68.
[19] Cui X, Mao S, Liu M, Yuan H, Du Y. Mechanism of surfactant micelle formation. Langmuir 2008;24:10771–5.
[20] Barnabas-Rodriguez R, Estelrich J. Photophysical changes of pyranine induced by surfactants: evidence of premicellar aggregates. Journal of Physical Chemistry B 2009;113:1972–82.
[21] Hadgiivanova R, Diamant H. Premicellar aggregation of amphiphilic molecules. Journal of Physical Chemistry B 2007;111:8854–9.
[22] Huang HS, Chiu HF, Yeh PF, Yuan CL. Structure-based design and synthesis of regioisomeric disubstituted aminoanthraquinone derivatives as potential anticancer agents. Helvetica Chimica Acta 2004;87:999–1006.
[23] Solodar WE, Kyriakakis BM. Rank Xerox Ltd. 1,5-Diaminoanthraquinone pigments and photoconductors. France patent FR 1484968. 1967 Jun 16.
[24] Cook AH, Waddington W. Experiments in the coeroxene and coeramidine series. Journal of the Chemical Society 1945;I:402–5.

[25] Jienifuaa K, Maatein J. BDH Chemicals Ltd. Multi-coloring dyestuff suitable for use dissolved in electro-optical apparatus. Japanese patent JP 54071088. 1979 Jun 7.
[26] Simon MS. Spectral shifts in anthraquinone dyes caused by non-conjugated substituents. Journal of the American Chemical Society 1963;85:1974–7.
[27] Barber DC, Freitag-Beeston RA, Whitten DG. Atropisomer-specific formation of premicellar porphyrin j-aggregates in aqueous surfactant solutions. Journal of Physical Chemistry 1991;95:4074–86.
[28] Ferreira JAB, Costar SMB. Rhodamine $3B^{+}ClO_4^{-}$ in water:toluene mixtures: evidence of water cluster formation. Chemical Physics Letters 1999;307:139–46.
[29] Antonious MS, Tada EB, El Seoud OA. Thermo-solvatochromism in aqueous alcohols: effects of the molecular structures of the alcohol and thesolvatochromic probe. Journal of Physical Organic Chemistry 2002;15:403–12.
[30] Guzow K, Milewska M, Wiczk W. Solvatochromism of 3-[2-(4-diphenylaminophenyl)benzoxazol-5-yl]alanine methyl ester: a new fluorescence probe. Spectrochimica Acta Part A 2005;61:1133–40.
[31] Lai WC, Dixit NS, Mackay RA. Formation of H aggregates of thionine dye in water. The Journal of Physical Chemistry 1984;88:5364–8.
[32] Reichardt C. Solvatochromic dyes as solvent polarity indicators. Chemical Reviews 1994;94:2319–58.
[33] Marcus Y. The properties of solvents. Chichester: Wiley; 1998. p. 140.
[34] Spange S, Prause S, Vilsmeier E, Thiel WR. Probing surface basicity of solid acids with an aminobenzodifurandione dye as the solvatochromic probe. The Journal of Physical Chemistry B 2005;109:7280–9.
[35] Wróblewska EK, Soroka JA, Soroka KB, Gasiorowska M. Solvatochromism of dyes. Part IV-Energetic characteristics of merocyanine derivatives of 1-phenyl-2-[2-(3-X-4-hydroxy-5-R-phenyl)ethenyl]-3,3-dimethyl-3 *H*-indolium cation. Journal of Physical Organic Chemistry 2005;18:347–52.
[36] Reichardt C. Solvents and solvent effects in organic chemistry. 3rd ed. Weinheim: Wiley-VCH; 2003. p. 17.
[37] Chen NL. Solvents handbook. 3rd ed. Beijing: Chemical Industrial; 2002.